






RESEARCH ARTICLE

The spermidine acetyltransferase SpeG regulates transcription of the small RNA *rprA*

Linda I. Hu¹[✉], Ekaterina V. Filippova²[✉], Joseph Dang³[✉], Sergii Pshenychnyi⁴, Jiapeng Ruan²[✉], Olga Kiryukhina², Wayne F. Anderson², Misty L. Kuhn³, Alan J. Wolfe¹^{*}

1 Department of Microbiology and Immunology, Loyola University Chicago, Health Sciences Division, Stritch School of Medicine, Maywood, IL, United States of America, **2** Center for Structural Genomics of Infectious Diseases, Northwestern University Feinberg School of Medicine, Department of Biochemistry and Molecular Genetics, Chicago, IL, United States of America, **3** Department of Chemistry and Biochemistry, San Francisco State University, San Francisco, CA, United States of America, **4** Recombinant Protein Production Core at Chemistry of Life Processes Institute, Northwestern University, Chicago, IL, United States of America

 These authors contributed equally to this work.

[✉] Current address: Department of Microbiology-Immunology, Feinberg School of Medicine, Northwestern University, Chicago, IL, United States of America

[✉] Current address: Department of Biochemistry and Molecular Biology, Knapp Center for Biomedical Discovery, University of Chicago, Chicago, IL, United States of America

[✉] Current address: Yale University School of Medicine, Department of Digestive Diseases, New Haven, CT, United States of America

* awolfe@luc.edu



 OPEN ACCESS

Citation: Hu LI, Filippova EV, Dang J, Pshenychnyi S, Ruan J, Kiryukhina O, et al. (2018) The spermidine acetyltransferase SpeG regulates transcription of the small RNA *rprA*. PLoS ONE 13 (12): e0207563. <https://doi.org/10.1371/journal.pone.0207563>

Editor: Fernando Rodrigues-Lima, Universite Paris Diderot, FRANCE

Received: October 30, 2018

Accepted: November 23, 2018

Published: December 18, 2018

Copyright: © 2018 Hu et al. This is an open access article distributed under the terms of the [Creative Commons Attribution License](https://creativecommons.org/licenses/by/4.0/), which permits unrestricted use, distribution, and reproduction in any medium, provided the original author and source are credited.

Data Availability Statement: All relevant data are within the manuscript and its Supporting Information files.

Funding: This project was funded by R01 GM066130 (NIGMS to AJW), R01 AI108255 (NIAID to AJW), by contracts HHSN272200700058C and HHSN272201200026C (NIAID, NIH, Department of Health and Human Services to WFA), and by startup funds from San Francisco State University (to MLK); NIGMS = National Institute of General Medical Sciences,

Abstract

Spermidine *N*-acetyltransferase (SpeG) acetylates and thus neutralizes toxic polyamines. Studies indicate that SpeG plays an important role in virulence and pathogenicity of many bacteria, which have evolved SpeG-dependent strategies to control polyamine concentrations and survive in their hosts. In *Escherichia coli*, the two-component response regulator RcsB is reported to be subject to N^ε-acetylation on several lysine residues, resulting in reduced DNA binding affinity and reduced transcription of the small RNA *rprA*; however, the physiological acetylation mechanism responsible for this behavior has not been fully determined. Here, we performed an acetyltransferase screen and found that SpeG inhibits *rprA* promoter activity in an acetylation-independent manner. Surface plasmon resonance analysis revealed that SpeG can physically interact with the DNA-binding carboxyl domain of RcsB. We hypothesize that SpeG interacts with the DNA-binding domain of RcsB and that this interaction might be responsible for SpeG-dependent inhibition of RcsB-dependent *rprA* transcription. This work provides a model for SpeG as a modulator of *E. coli* transcription through its ability to interact with the transcription factor RcsB. This is the first study to provide evidence that an enzyme involved in polyamine metabolism can influence the function of the global regulator RcsB, which integrates information concerning envelope stresses and central metabolic status to regulate diverse behaviors.

<https://www.nigms.nih.gov/>; NIAID = National Institute of Allergy and Infectious Diseases, <https://www.niaid.nih.gov/>; SFSU = San Francisco State University, <http://www.sfsu.edu/>. The funders had no role in study design, data collection and analysis, decision to publish, or preparation of the manuscript.

Competing interests: The authors have declared that no competing interests exist.

Introduction

SpeG, a member of the Gcn5-related *N*-acetyltransferase (GNAT) family, is a bacterial spermidine *N*-acetyltransferase that acetylates spermidine and spermine. These polyamines are toxic to bacteria at high concentrations and acetylation neutralizes this toxicity [1, 2]. Studies indicate that SpeG plays an important role in virulence and pathogenicity of many bacteria, which have evolved SpeG-dependent strategies to control polyamine concentrations and survive in their hosts [3–6]. Kinetic and structural analyses have demonstrated that SpeG from both *Escherichia coli* and *Vibrio cholerae* can acetylate spermidine [7–9]. These studies also showed that SpeG from *V. cholerae* is an allosteric protein; when spermidine binds to its allosteric site, SpeG exhibits a symmetric closed dodecameric structure [7, 9]. Finally, in the absence of spermidine binding, *V. cholerae* SpeG can adopt a unique asymmetric dodecameric structure with an open conformational state [10].

During the course of this study, we found that SpeG also regulates the small RNA *rprA*, whose transcription strictly requires the phosphorylated isoform of the two-component response regulator RcsB [11, 12]. The canonical two-component signal transduction system is composed of two proteins. The first is a sensor kinase that detects a signal and, in response, autophosphorylates a conserved histidine residue using ATP as the phosphoryl donor. The second is a response regulator that autophosphorylates a conserved aspartate residue using the phosphorylated sensor kinase as the phosphoryl donor [for reviews, see [13–15]]. A more complex variant of the basic two-component system is the phosphorelay, such as the Rcs phosphorelay, which consists of five proteins (RcsC, RcsD, RcsF, IgaA, and RcsB). The first four proteins are involved in controlling the phosphorylation status of the response regulator RcsB in response to diverse extracytoplasmic stimuli. The phosphorylation status of RcsB is set by an ATP-dependent protein-protein interaction chain whose core consists of the cytoplasmic membrane-associated sensor kinase/phosphatase RcsC and its cognate histidine phosphotransferase RcsD [16]. The inner membrane protein IgaA favors RcsC phosphatase activity and thus dephosphorylation of RcsB. Relocation of the outer membrane lipoprotein RcsF to the periplasm favors RcsC kinase activity and thus phosphorylation of RcsB. This occurs when RcsF interacts with the C-terminal periplasmic domain of IgaA. Together, RcsF and IgaA regulate the activities of the Rcs phosphorelay components [17–24]. RcsB also can become phosphorylated in response to central metabolic changes via the central metabolite acetyl phosphate [25]. Both mechanisms (RcsC-dependent and acetyl phosphate-dependent) regulate the phosphorylation status of RcsB and thus both control RcsB-dependent processes, such as desiccation, flagellar biogenesis, capsule biosynthesis, and cell division [16, 25–28].

The Rcs phosphorelay is unusual, as the response regulator RcsB can form both a homodimer and a variety of heterodimers. The homodimer activates transcription of *rprA* [11, 12, 29], which encodes the small RNA regulator of the stationary phase sigma factor RpoS, and represses transcription of *flhDC*, which encodes the master regulator of the flagellar regulon [25, 30, 31]. In the absence of RcsB, *rprA* mRNA is not detectable by Northern blot analysis [12] and *rprA* promoter activity is diminished by almost two logs [29]. Thus, *rprA* transcription is considered to be strictly dependent on RcsB. To activate synthesis of the capsular exopolysaccharide colanic acid, RcsB forms a complex with a partner transcription regulator, RcsA, stabilizing the interaction between RcsB and a specific DNA binding site, the “RcsAB box” [32, 33]. RcsB also can form protein-protein complexes with other partner transcription factors, including GadE, RmpA, MatA, BglJ, and RflM; there is also evidence to suggest an interaction with PhoP [34–39]. Because these protein-protein complexes form in response to a variety of conditions, the Rcs system can mediate diverse responses that contribute to biofilm formation, virulence, motility and antibiotic resistance in pathogens [26–28, 34–36].

Biochemical and mass spectrometry analyses indicate that RcsB can become N^ε-lysine acetylated on multiple residues [29, 40–42]. Two mechanisms for N^ε-lysine acetylation have been reported. One mechanism involves the direct donation of the acetyl group from acetyl phosphate to a deprotonated lysine ε-amino group [41, 43]. The other mechanism is enzymatic, relying on a lysine acetyltransferase (KAT) to catalyze donation of the acetyl group from acetyl-coenzyme A (acCoA) to the ε-amino group of a lysine residue [44]. All known bacterial KATs are members of the large family of GNATs [29, 40, 44–47].

One of our previous studies suggested that acetylation of RcsB diminished its ability to activate *rprA* transcription in *E. coli* [29]. In an effort to identify a KAT that might affect RcsB acetylation, we first screened 21 known *E. coli* genes that encode or are predicted to encode GNATs, seeking those that inhibited the RcsB-dependent *rprA* transcription. This screen revealed that SpeG could inhibit *rprA* activity; however, we obtained no evidence that SpeG functions as a RcsB lysine N^ε-acetyltransferase. Instead, we report here that SpeG can interact with RcsB through the latter’s DNA binding domain. Our findings represent the first evidence that the metabolic enzyme SpeG can affect transcription by interacting with the response regulator RcsB.

Results

SpeG regulates *rprA* promoter activity

While the GNAT YfiQ (also known as Pka and PatZ) can acetylate RcsB *in vitro* [29, 40], the *yfiQ* mutant does not affect RcsB acetylation [29]. Therefore, we suspected another GNAT was responsible for RcsB acetylation and proceeded to test a series of 21 known or putative GNATs. We overexpressed these GNATs and measured their effect on *PrprA-lacZ*, a transcriptional fusion of the RcsB-dependent *rprA* promoter (*PrprA*) and the *lacZ* gene, which we had integrated as a single copy into the chromosome of BW25113 to generate our reference strain AJW3759 (Table 1) [12]. From this preliminary screen, we identified SpeG as an inhibitor of

Table 1. Bacterial strains, bacteriophage, plasmids, and primers used in this study.

Strain, phage, plasmid, or primer	Relevant Characteristic	Source/Reference
Strains		
BW25113	F ⁻ λ- Δ(<i>araD-araB</i>)567 Δ(<i>rhaD-rhaB</i>)568 Δ <i>lacZ</i> 4787 <i>rrnB3 rph-1 hsdR514</i>	[48]
AJW3759	BW25113 λΦ(<i>PrprA142-lacZ</i>)	λ: λ <i>rprA142</i> → BW25113
AJW4589	AJW3759 Δ <i>speG::FRT</i>	P1: JW1576 [49] → AJW3759, then removed antibiotic marker
AJW4533	AJW3759 Δ <i>speE::FRT</i>	P1: JW0117 [49] → AJW3759, then removed antibiotic marker
BL21 (DE3) Magic	Competent cells; a derivative of BL21 cells carrying a plasmid encoding rare tRNAs; Kn ^R	[50]
Phage		
λ <i>rprA142</i>	<i>rprA142-lacZ</i>	[12]
Plasmids		
pCA24n	Control plasmid: Cm ^R	[51]
pMCSG7	pET21 derivative for ligation independent cloning; adds N-terminal His tag and TEV cleavage site; Ap ^R	[52]
pMCSG53	pET21 derivative for ligation independent cloning; adds N-terminal His tag and TEV cleavage site; Ap ^R	[53]
pCA24n- <i>rscB</i>	JW4054; IPTG-inducible His ₆ -RcsB expression; Cm ^R	[51]
pCA24n- <i>speG</i>	JW1576; IPTG-inducible His ₆ -SpeG expression; Cm ^R	[51]
pCA24n- <i>speG</i> (Y135A)	Site-directed mutagenesis of pCA24n- <i>speG</i> to carry an alanine at amino acid 135.	This study

(Continued)

Table 1. (Continued)

Strain, phage, plasmid, or primer	Relevant Characteristic	Source/Reference
pMCSG7- <i>rbsB</i> (NTD)	pMCSG7 expressing His ₆ -RcsB (residues1-147); Ap ^R	This study
pMCSG7- <i>rbsB</i> (CTD)	pMCSG7 expressing His ₆ -RcsB (residues128-216); Ap ^R	This study
pMCSG53- <i>rbsA</i> pMCSG7- <i>speG</i>	pMCSG53 expressing His ₆ -RcsA (residues 4–207); Ap ^R pMCSG7 expressing His ₆ -SpeG; Ap ^R	[7]
Primers (5'-3')		
<i>rbsB</i> (CTD)_F	AAGGAGATATACATATGCATCACCATCACCACCATAAATTCACACCGGAGAGCG	This study
<i>rbsB</i> (CTD)_R	AAGTACAGGTTCTCGGTACCTTATTAGTCTTTGTCCGCCGAGAC	This study
<i>rbsB</i> (NTD)_F	AAGGAGATATACATATGCACCATCATCACCACCATAACAACATGAACGTTATTATCGCAGATGAC	This study
<i>rbsB</i> (NTD)_R	AAGTACAGGTTCTCGGTACCTTATTAGCCATAGCCGCCTGCAG	This study
SDM _{speGY135A}	AAAGCCAAGCTTGCAGGCAATGTGAATCGCTTTTTTCATTCTCTTTATCA	This study
SDM _{speGY135A_as}	TGATAAAGAGAATGAAAAAGCGATTTCACATTGCCCGCAAGCTTGGCTTT	This study

<https://doi.org/10.1371/journal.pone.0207563.t001>

PrprA activity. When SpeG was overexpressed from a plasmid in the reference strain, *PrprA* activity was reduced compared to the vector control during late exponential growth and during the transition into early stationary phase (OD > 1.0, Fig 1A, linear regression analysis $t = -2.553$, $p = 0.01472$). When *speG* was deleted, *PrprA* activity increased in the isogenic *speG* mutant compared to its wild-type parent (Fig 1B, linear regression analysis $t = 7.750$, $p = 8.65E-12$). Based on these results, we conclude that SpeG inhibits transcription from *PrprA*.

SpeG does not acetylate RcsB *in vitro*

Since SpeG belongs to the GNAT family of acetyltransferases known to acetylate proteins, we also tested the hypothesis that SpeG regulates *rprA* transcription by acetylating RcsB. To accomplish this, we used an *in vitro* colorimetric enzymatic assay with purified recombinant proteins. This assay measures the formation of product (CoA) indirectly via its reaction with dithionitrobenzoic acid (DTNB) to produce the thioanion product thionitrobenzoate (TNB²⁻), which is monitored spectrophotometrically at 415 nm [7, 54]. We compared the acetylation activity of SpeG toward spermidine or RcsB. As predicted, we detected SpeG acetylation activity on spermidine when acCoA was present; however, we observed no change in RcsB acetylation status in the presence of SpeG and acCoA (Fig 2). This result suggests that RcsB is not a substrate for SpeG under the conditions we used to assay acetylation.

Spermidine synthase (SpeE) is not required for SpeG-dependent inhibition of *rprA* transcription

The spermidine synthase SpeE transfers a propylamine from decarboxylated S-adenosyl-methionine to putrescine to form spermidine, which is both a substrate and an allosteric activator of SpeG [7]. To explore the role of SpeE/spermidine in SpeG overexpression-inhibited *PrprA* activity, we transformed a mutant that does not synthesize spermidine (*speE*) and its WT parent with either the SpeG overexpression plasmid or its vector control and monitored *PrprA* activity (Fig 3). SpeG overexpression resulted in reduced *PrprA* activity in both the parental strain (Fig 3, linear regression analysis $t = -3.752$, $p = 0.000282$) and the *speE* mutant (Fig 3, linear regression analysis $t = -3.470$, $p = 0.000745$). Furthermore, exposure of the *speE* mutant to exogenous spermidine exerted no effect on *PrprA* activity whether or not SpeG was overexpressed (S1 Fig). We conclude that SpeG can inhibit *PrprA* activity regardless of SpeE/spermidine status.

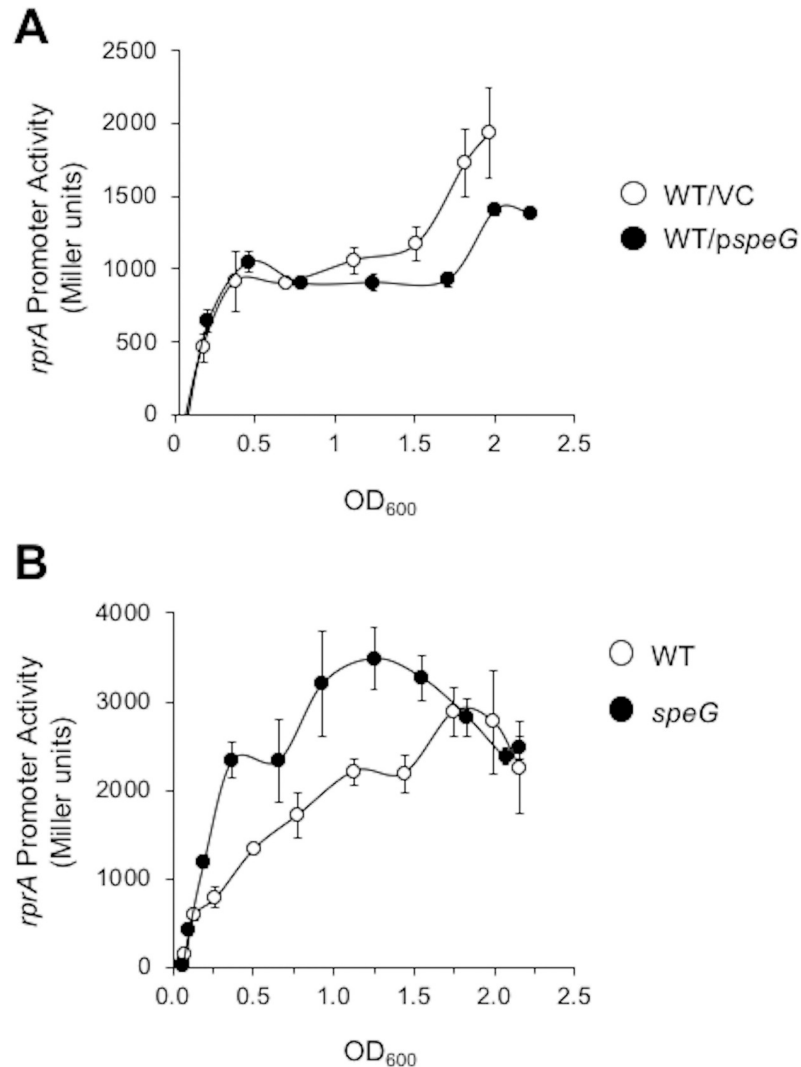


Fig 1. The effect of SpeG on *rprA* promoter activity A. WT cells carrying the *PrprA-lacZ* fusion (AJW3759) were transformed with either a plasmid that expresses SpeG under the control of an IPTG-inducible promoter (*pspeG*; pCA24n-*speG*) or the vector control (VC; pCA24n) and grown in TB7 containing 50 μ M IPTG to induce SpeG expression and chloramphenicol to maintain the plasmid. Cell growth and β -galactosidase activity were assayed at various points throughout growth. The values represent average promoter activity with standard deviations of triplicate independent cultures. Linear regression analysis of the experimental group WT/*pspeG* on *rprA* promoter activity versus WT/VC was statistically significant ($t = -2.553$, $p = 0.01472$). B. WT (AJW3759) and isogenic *speG* (AJW4589) strains were assayed for cell growth in TB7 and β -galactosidase activity. The values represent average promoter activity with standard deviations of five independent WT and *speG* cultures. Linear regression analysis of the experimental group *speG* on *rprA* promoter activity versus WT was statistically significant ($t = 7.750$, $p = 8.65E-12$).

<https://doi.org/10.1371/journal.pone.0207563.g001>

Catalytic activity of SpeG is not required for SpeG-dependent inhibition of *rprA* transcription

We next asked if SpeG overexpression-dependent inhibition of *PrprA* activity requires the spermidine acetyltransferase activity of SpeG. We therefore overexpressed SpeG Y135A, a predicted catalytically inactive SpeG variant, in the parent (AJW3759). This tyrosine (Y) residue acts as a general acid during substrate acetylation and has been shown to be critical for catalytic activity of many GNAT homologs [55–57]. We found that the SpeG Y135A mutant retained the ability to inhibit *PrprA* activity in the parent AJW3759 (Fig 3A, linear regression

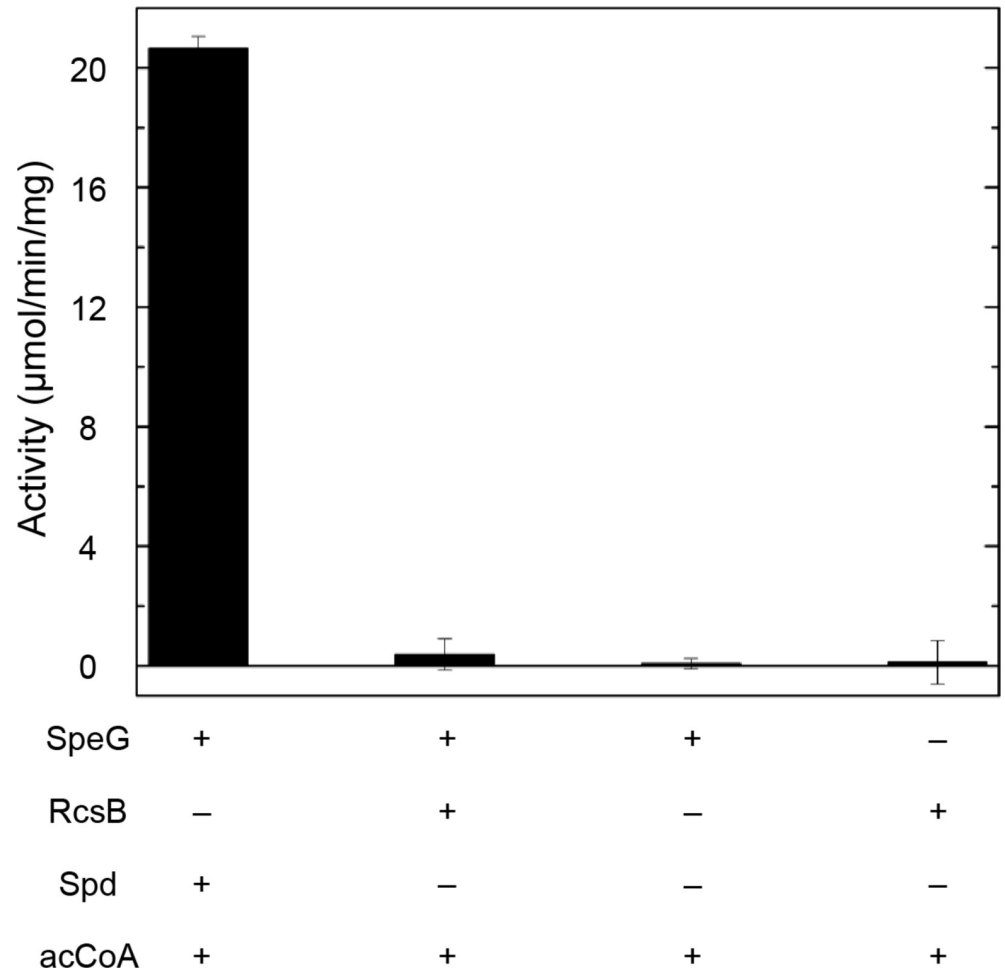


Fig 2. *In vitro* acetylation activity of SpeG toward RcsB or spermidine. SpeG was incubated with either spermidine or RcsB in the presence of the acetyl donor acCoA to determine if SpeG uses both spermidine and RcsB as substrates. Control reactions of possible non-enzymatic acetylation of SpeG and RcsB via acCoA were also performed. See [Materials and Methods](#) for specific reaction conditions.

<https://doi.org/10.1371/journal.pone.0207563.g002>

analysis $t = -2.456$, $p = 0.015623$). These results are consistent with a SpeG-dependent, but spermidine acetylation-independent mechanism of inhibition in WT cells.

SpeG binds to RcsB through its C-terminal domain

Since SpeG does not appear to acetylate RcsB and its catalytic activity is unnecessary for its ability to inhibit *rprA* transcription, we considered whether SpeG inhibits RcsB activity through a physical interaction. We used SPR to investigate whether SpeG and RcsB can form a complex. First, we immobilized SpeG onto the SPR chip and evaluated whether full-length RcsB or its N- or C-terminal domains could bind to SpeG. Both full-length RcsB (Fig 4A) and its C-terminal domain (Fig 4B) bound to immobilized SpeG in a concentration-dependent manner. In contrast, the N-terminal domain of RcsB did not (Fig 4C). These results suggest that RcsB binds to SpeG through its C-terminal domain. We also performed the reverse experiment, assessing whether SpeG could bind to immobilized RcsB or its domains, but we detected no signal. Perhaps RcsB binds to the chip in a manner that prevents interaction with SpeG.

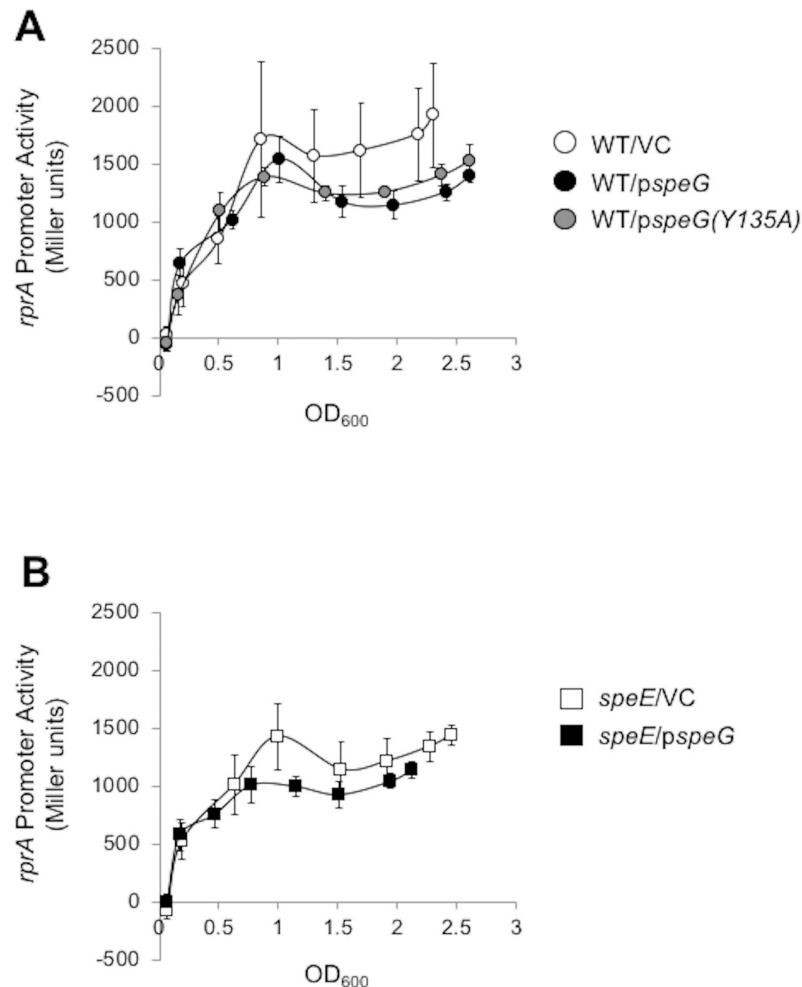


Fig 3. The effect of overexpressing SpeG or SpeG(Y135A) in WT cells and overexpressing SpeG in the *speE* mutant on *rprA* promoter activity. A. WT cells carrying the *PrprA-lacZ* fusion (AJW3759) were transformed with either *pspeG* (pCA24n-*speG*), *pspeG(Y135A)* (pCA24n-*speG(Y135A)*), or the VC (pCA24n) and grown in TB7 supplemented with 50 μ M IPTG and chloramphenicol to maintain the plasmid. Cell growth and β -galactosidase activity were assayed. The values represent average promoter activity with standard deviations of five independent cultures. B. The isogenic *speE* mutant was transformed with either *pspeG* (pCA24n-*speG*) or the VC (pCA24n) and cell growth and β -galactosidase activity were assayed as described for 3A. The values represent average promoter activity with standard deviations of five independent cultures. Linear regression comparison results on *rprA* promoter activity were significant for all experimental groups: WT/*pspeG* versus WT/VC ($t = -3.752$, $p = 0.000282$), WT/*pspeG(Y135A)* versus WT/VC ($t = -2.456$, $p = 0.015623$), and *speE/pspeG* versus *speE/VC* ($t = -3.470$, $p = 0.000745$).

<https://doi.org/10.1371/journal.pone.0207563.g003>

We calculated a K_D of 67 μ M for the binding of SpeG to the RcsB C-terminal domain from the fit to a simple one-to-one binding model, in which one C-domain RcsB molecule interacts with one SpeG molecule (S2A Fig). However, we could not determine the K_D for the SpeG/full-length RcsB interaction, as the data did not fit either a simple binding model or other models defined in the SPR data analysis software program TraceDrawer. The lack of fitting for the SpeG/full-length RcsB interaction likely resulted from the pronounced peak at the beginning of the sensograms, which occurred especially with higher concentrations of RcsB.

We next tested the effect of spermidine on the SpeG-RcsB interaction. To accomplish this, we exposed the surface of the chip containing immobilized SpeG to spermidine and then measured the SPR signal from binding the three separate RcsB constructs (described in Materials

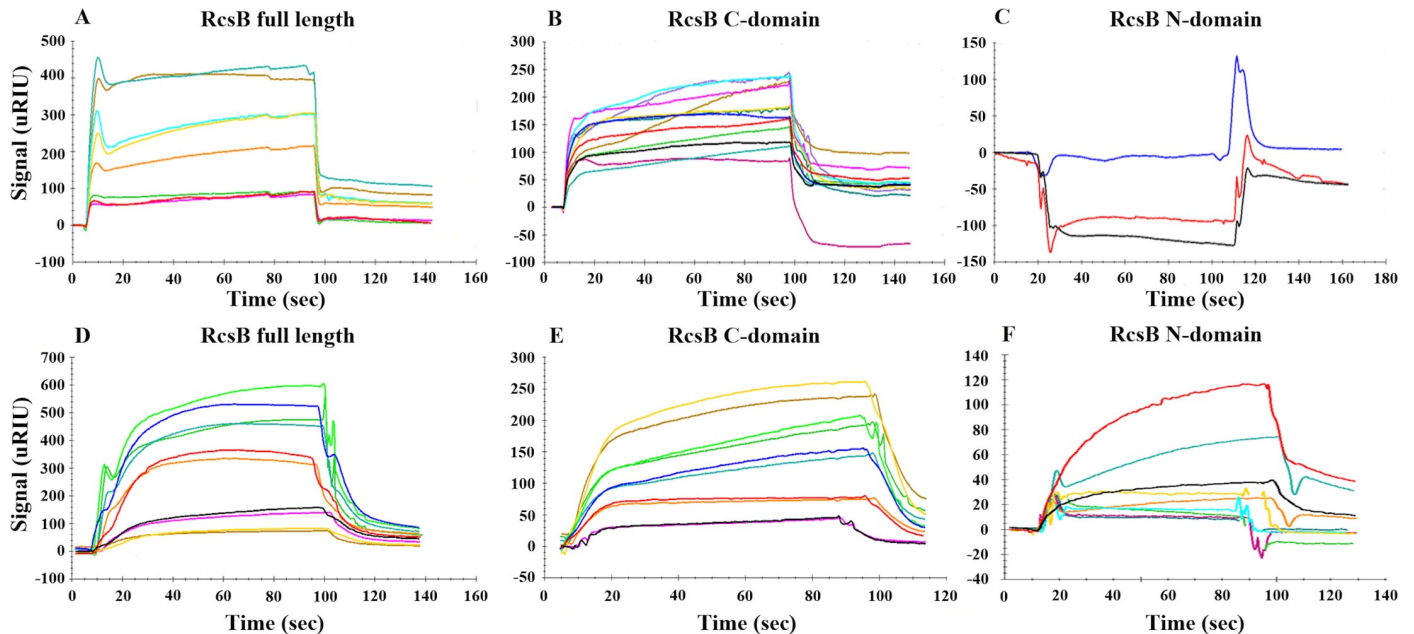


Fig 4. SPR analysis of the SpeG-RcsB interaction. The dose-response analysis for immobilized *E. coli* SpeG (46 μ M) with increasing concentrations of full-length *E. coli* RcsB (21, 42, 53, 63 and 74 μ M) as an analyte in the absence of spermidine (A) or RcsB (21, 42, 53, 63 and 74 μ M) after exposure to 0.5 mM spermidine (D), RcsB C-terminal domain (45, 67, 91, 114, 136, and 159 μ M) in the absence of spermidine (B) or RcsB C-terminal domain (23, 45, 91, 114, and 136 μ M) after exposure to 0.5 mM spermidine (E), and RcsB N-terminal domain (59, 118, and 176 μ M) in the absence of spermidine (C) or RcsB N-terminal domain (59, 118, 177, 236 and 295 μ M) after exposure to 0.5 mM spermidine (F).

<https://doi.org/10.1371/journal.pone.0207563.g004>

and Methods; Fig 4D–4F). By fitting the sensorgrams to these data using the one-to-one binding model, we obtained K_D values of 128 and 281 μ M for the RcsB full-length and its C-terminal domain, respectively (S2B and S2C Fig). In contrast, we could not determine a K_D for the RcsB N-terminal domain due to a large chi-squared fitting value. Furthermore, we conclude that the binding of the N-terminal domain to SpeG is weak because the response signals obtained at concentrations greater than 100 μ M were relatively low (Fig 4F). On the basis of these data and those obtained in the absence of spermidine, we propose that SpeG interacts with the C-terminal domain of RcsB in the presence or absence of spermidine and that spermidine does not prevent RcsB binding to SpeG.

Possible SpeG inhibition of LuxR/FixJ-like transcription factors

SpeG inhibits *rprA* transcription and binds RcsB through the carboxyl terminal domain, which contains the conserved DNA binding helix-turn-helix (HTH) motif found in RcsB and other LuxR/FixJ-type proteins [16, 58]. Based on this result, it is tempting to speculate that SpeG may also bind other LuxR/FixJ family members. To identify conserved residues of the RcsB HTH motif across other LuxR/FixJ-like transcriptional regulators from *E. coli*, we used the PSI-BLAST server [59] to generate a list of DNA-binding domains from LuxR/FixJ-type family homologs and the NMR structure of the RcsB C-terminal domain from *Erwinia amylovora*, a close relative of *E. coli* [32] to visualize sequence conservation with respect to the three-dimensional structure (Fig 5). We also generated a phylogenetic tree using these sequences to determine which RcsB homologs had the greatest sequence similarity to its C-terminal domain and, therefore, propensity for interacting with SpeG (S3 Fig). We found the most conserved RcsB C-terminal domain residues across LuxR/FixJ-type homologs are S152, P153, K154, L167, V168, T169, R177, S178, K180, T181, S183, S184, Q185, K186, K187, and D198. From

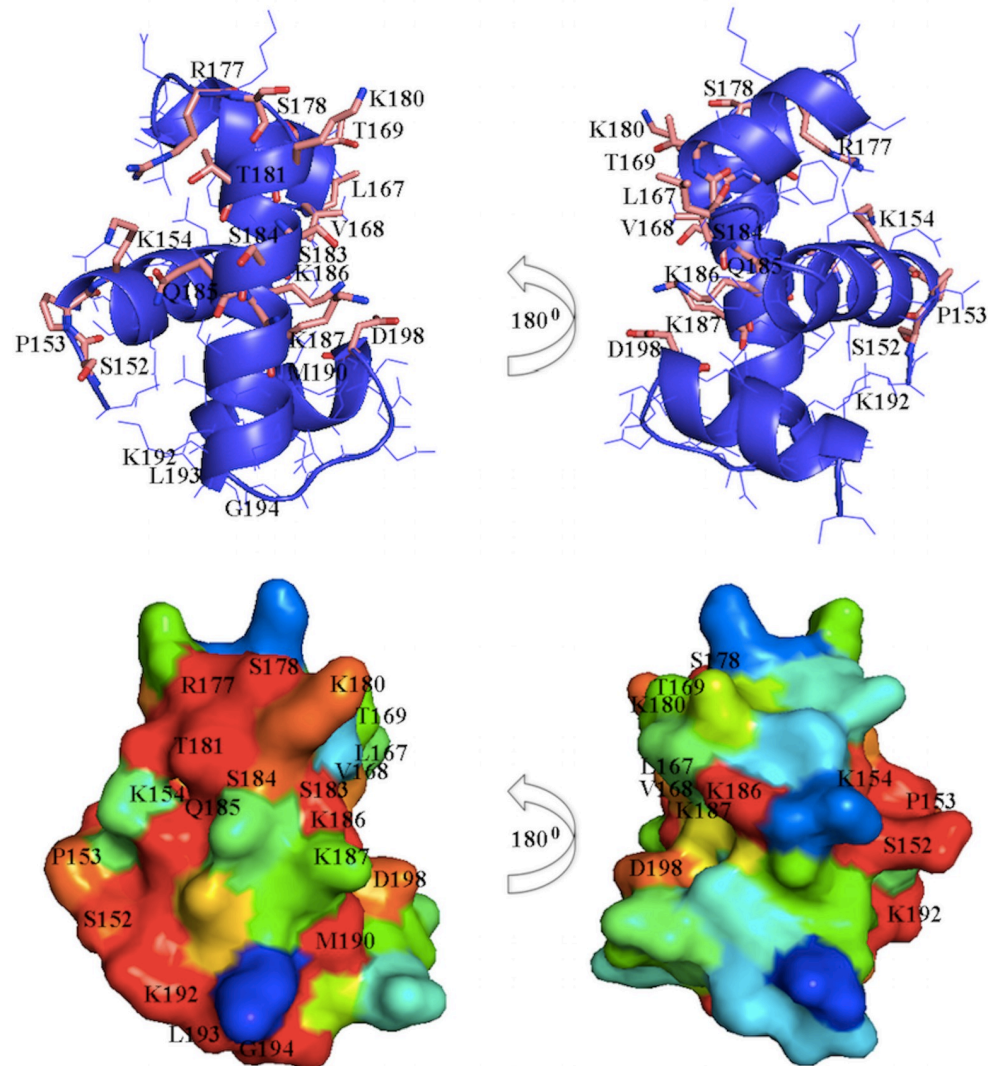


Fig 5. Structure analysis of the RcsB C-terminal DNA-binding domain. Ribbon diagram of the RcsB C-terminal DNA-binding domain from *Erwinia amylovora* (top panel). Conserved residues involve in DNA contacts in known LuxR/FixJ regulators are shown as stick models. RcsB DNA-binding domain: sequence-structure alignment (bottom panel). Surface representation of the RcsB DNA-binding domain was colored by the degree of sequence conservation from red (100% conserved residues) to blue (non-conserved residues). A search for RcsB C-terminal DNA-binding domain homologs was done using the PSI-BLAST server. From the list of 500 sequences against the non-redundant database a random set of 30 sequences with identity from 98% to 40% were chosen. A multiple sequence alignment for visualization of the sequence conservation with respect to the three-dimensional structure was generated.

<https://doi.org/10.1371/journal.pone.0207563.g005>

our analysis, the *E. coli* LuxR/FixJ-type homolog sequences of YjjQ, BglJ, YahA, YuaB, DctR, and RcsA are most similar to the RcsB C-terminal DNA-binding domain and warrant further testing. We hypothesized that SpeG might bind RcsB through these critical residues in the C-terminal domain and potentially those of other homologs.

SpeG does not bind the LuxR/FixJ family member RcsA

To determine if binding to SpeG is specific for RcsB or if SpeG can bind *in vitro* to other LuxR/FixJ transcriptional regulators that have C-terminal domains similar to RcsB, we heterologously expressed and purified the *E. coli* RcsA transcriptional regulator (an auxiliary

partner with RcsB in a heterodimer that interacts with a specific DNA site called the “RcsAB” box [60]) and tested RcsA binding to SpeG by SPR. We found that SpeG does not bind to RcsA in the absence of spermidine (S4 Fig), which highlights the binding specificity between RcsB and SpeG. However, we cannot exclude that possibility that SpeG may bind an RcsB-RcsA heterodimer or other LuxR/FixJ-type family members in the presence or absence of spermidine. While RcsA has an HTH motif, its inability to bind SpeG also suggests that other regions of RcsB within its DNA-binding domain besides the HTH motif and/or its oligomeric state might be important for the specificity of the SpeG-RcsB interaction.

Discussion

We have presented evidence that the metabolic enzyme SpeG regulates transcription from the *rprA* promoter. We also have shown that SpeG binds the DNA binding domain of the transcription factor RcsB. We propose that this interaction interferes with the ability of RcsB to activate transcription from the *rprA* promoter. This represents the first report of a direct link between spermidine metabolism and an envelope stress signal transduction pathway.

SpeG can inhibit *rprA* transcription through interactions with RcsB

We began this study because we had previously reported that N^ε-lysine acetylation regulates RcsB activity at the *rprA* promoter [29]. Since deletion of the only known *E. coli* N^ε-lysine acetyltransferase YfiQ had no obvious effect on the acetylation state of RcsB [29], we screened the known and putative acetyltransferases for regulators of *rprA* transcription and found that SpeG inhibited *rprA* promoter activity: overexpression of SpeG reduced *rprA* promoter activity (Fig 1A), while deleting *speG* relieved inhibition of the *rprA* promoter (Fig 1B).

Because we did not observe acetylation of RcsB by SpeG (Fig 2) and since we did not find that SpeG activity could affect RcsB-dependent *rprA* inhibition (Fig 3), we instead investigated the possibility of a physical interaction between RcsB and SpeG. Indeed, SPR analysis showed that SpeG forms a complex with RcsB through the RcsB C-terminal DNA-binding domain (Fig 4). We further report that this interaction is specific, as we did not detect binding between SpeG and RcsB's auxiliary transcription factor RcsA (57) (S3 and S4 Figs). These *in vitro* results combined with the *in vivo* analysis support the hypothesis that SpeG and RcsB interact and that the resulting complex impacts RcsB activity at the *rprA* promoter. As *rprA* transcription absolutely requires RcsB, we did not test if SpeG affected *rprA* transcription in an *rpsB* mutant.

Physiological implications of SpeG-RcsB interactions

It has been estimated that RcsB regulates 5% of the *E. coli* genome, including but not limited to the colanic acid biosynthetic locus, the small RNA *rprA*, and the operon that encodes FlhDC, the master regulator of flagellar biogenesis [61, 62]. The Rcs phosphorelay has also been implicated in regulating biofilm formation and sensitivity to antibiotic-induced peptidoglycan damage [16, 62–64]. Since the SpeG interaction with RcsB regulates activation of *rprA* transcription, SpeG likely influences these other RcsB-regulated phenotypes. In fact, it has been reported that polyamines can induce the glutamate-dependent acid response system [65], which requires RcsB [66]. The outstanding question is why polyamine neutralization and cellular processes regulated by RcsB would be coordinated. We conjecture that SpeG works through members of the RcsB regulon required to initiate proper responses to particular extracellular conditions such as cold shock, heat shock, ethanol, and increased alkalinity, which were shown to influence the spermidine metabolic pathway [67].

Conclusion

We have shown that SpeG and RcsB can form a complex, suggesting a coordinated response between polyamine metabolism and envelope stress. It is not known why an enzyme involved in spermidine metabolism regulates RcsB, if RcsB affects spermidine biosynthesis, or whether SpeG acts as a general modulator of response regulators. However, it is clear that SpeG inhibits RcsB activity *in vivo* and we propose that it is through a direct interaction between SpeG and the DNA binding domain of RcsB.

Materials and methods

Bacterial strains, bacteriophage, and plasmids

All of the bacterial strains, bacteriophage, and plasmids used in this study are listed in [Table 1](#). Derivatives were constructed by generalized transduction with P1kc [68]. *PrprA142-lacZ*, a transcriptional fusion of the *rprA* promoter (*PrprA*) to the *lacZ* reporter, was from Dr. Susan Gottesman (National Institutes of Health, Bethesda, MD) [12]. Construction of monolysogens was performed and verified as described previously [69]. Transformations were performed by electroporation or through the use of either transformation buffers 1 and 2 [70] or transformation-and-storage solution [71].

Culture conditions

For strain construction, cells were grown in lysogeny broth (LB) consisting of 1% (w/v) tryptone, 0.5% (w/v) yeast extract, and 0.5% (w/v) sodium chloride; LB plates contained 1.5% agar. For promoter activity assays, cells were grown in tryptone broth buffered at pH 7 (TB7), which contains 1% (w/v) tryptone buffered at pH 7.0 with potassium phosphate (100 mM). Cell growth was monitored spectrophotometrically (DU640; Beckman Instruments, Fullerton, CA) by determining the absorbance at 600 nm (OD_{600}). Chloramphenicol (25 μ g/ml) was added to growth media when needed to maintain pCA24n plasmid derivatives. To induce the expression of genes carried on various plasmids, 10 μ M isopropyl- β -D-thiogalactopyranoside (IPTG) was added to the growth media.

β -galactosidase assay

To monitor the promoter activity of *PrprA-lacZ*, biological replicates were grown aerobically at 37°C in TB7 overnight. The overnight cultures were diluted in fresh TB7 to an OD_{600} of 0.05 and grown aerobically with agitation at 250 rpm at 37°C until early stationary phase. At regular intervals, cells were harvested and stored at 4°C in a microtiter plate. β -galactosidase activity was determined quantitatively as described previously (26) using All-in-One β -galactosidase reagent (Pierce Biochemical). Sterile TB7 was used as a negative control on each microtiter plate. Promoter activity was monitored throughout growth and plotted against OD_{600} . Each individual experiment included at least three biological replicates. Each of these experiments was performed at least three times. The values represent the means with standard deviations.

Site-directed mutagenesis

Site-directed mutagenesis of SpeG to pCA24n-speG(Y135A) was conducted in pCA24n-speG with the QuikChange Lightning Multi site-directed mutagenesis kit (Agilent Technologies), in accordance with the manufacturer's instructions by using the mutagenic primers SDMspeGY135A and SDMspeGY135A_as, as listed in [Table 1](#).

RcsB, RcsA and SpeG expression plasmids

Plasmids containing genes from *Escherichia coli* str. K-12 substr. MG1655 included the following: 1) full-length RcsB (NCBI accession code AAC75277, GI: 1788546) in the pCA24n vector from the ASKA collection (chloramphenicol resistant; pCA24n-*rcsB*) [51], 2) the N-terminal receiver domain of RcsB (truncated construct, residues 1–147) in the pMCSG7 vector (ampicillin resistant; pMCSG7-*rcsB*(NTD)), 3) the C-terminal DNA binding domain of RcsB (truncated construct, residues 128–216) in the pMCSG7 vector (ampicillin resistant; pMCSG7-*rcsB*(CTD)), 4) full-length RcsA (NCBI accession code WP_000104001 and GI: CTS77413) in the pMCSG53 vector (ampicillin resistant; pMCSG53-*rcsA*) and 5) full-length SpeG (NCBI accession code NP_416101, GI: 16129542) in the pMCSG7 vector (ampicillin resistant; pMCSG7-*speG*). The full-length RcsB construct (pCA24n-*rcsB*) and its truncated versions ((pMCSG7-*rcsB*(NTD) and pMCSG7-*rcsB*(CTD)) had an uncleavable N-terminal polyhistidine tag, while the RcsA (pMCSG53-*rcsA*) and SpeG (pMCSG7-*speG*) constructs had a cleavable N-terminal polyhistidine tag followed by a TEV protease cleavage site [51]. The genes for the individual RcsB domains were synthesized by Genescript and subcloned into the pMCSG7 vector using ligation independent cloning as described previously [72, 73]. A portion of the linker sequence (comprised of residues 121–149) between the domains was included in each individual domain construct.

Large-scale protein expression and purification

Expression plasmids containing the desired genes were transformed into kanamycin-resistant BL21(DE3)-magic or KRX/pGro7 (for pMCSG53-*rcsA*) competent cells [74]. pCA24n-*rcsB* transformants were grown in Terrific Broth (TB) in the presence of 34 µg/mL chloramphenicol and 35 µg/mL kanamycin. pMCSG7-*rcsB*(NTD) and pMCSG7-*rcsB*(CTD) transformants were grown in LB in the presence of 400 µg/mL ampicillin and 25 µg/mL kanamycin. The pMCSG53-*rcsA* transformant was grown in M9 L-selenomethionine supplemented media (Medicilon Inc.) in the presence of 400 µg/mL ampicillin, 35 µg/mL kanamycin and 0.1% arabinose. pMCSG7-*speG* transformants were grown in TB supplemented with 100 µg/mL ampicillin and 50 µg/mL kanamycin.

Full-length RcsB protein, its N-terminal and C-terminal domains, and RcsA protein were prepared at the Recombinant Protein Production Core (rPPC) Facility at Northwestern University (Evanston, IL, USA). Transformants containing the RcsB and RcsA plasmids were grown at 37°C in a fermenter until the OD₆₀₀ reached 0.8, whereupon they were induced with 0.6 mM IPTG. The RcsA transformant was also exposed to 0.25% L-rhamnose. The RcsB constructs were expressed at 25°C overnight, whereas RcsA was expressed at 22°C overnight. The next day cells were harvested by centrifugation and resuspended in lysis buffer (1.5 mM magnesium acetate, 1mM calcium chloride, 250 mM sodium chloride, 100 mM ammonium sulfate, 40 mM disodium phosphate, 3.25 mM citric acid, 5% glycerol, 5 mM imidazole, 5 mM beta-mercaptoethanol (BME), 0.08% n-dodecyl-beta-maltoside (DDM), 1 mM phenylmethylsulfonyl fluoride (PMSF), and 20 µM leupeptin) and homogenized. Cells containing the SpeG plasmid were grown at 37°C in a benchtop shaker to an OD₆₀₀ of 0.6, induced with 0.5 mM IPTG, and expressed at 25°C overnight. Cells were harvested and resuspended in lysis buffer (as stated above without PMSF and leupeptin) and sonicated. After sonication, lysates were centrifuged and the supernatant was purified as follows.

The proteins were purified using an ÄKTAexpress (GE Healthcare, Piscataway, NJ) high-throughput purification system at 4°C. The crude extract was loaded onto a 5 mL HisTrap FF Ni-NTA column, washed with loading buffer (10 mM Tris HCl pH 8.3, 500 mM sodium chloride and 5 mM BME), washed with loading buffer plus 25 mM imidazole to remove impurities,

and eluted with loading buffer plus 500 mM imidazole. The purified proteins were subsequently loaded onto and eluted from a HiLoad 26/60 Superdex 200 size-exclusion column in loading buffer. The polyhistidine tag of the SpeG protein was removed, as described previously [75]; for all other constructs, the tag remained attached. The final purity of each protein was assayed by SDS-PAGE.

Enzyme kinetic assays

To test whether SpeG could acetylate RcsB, we performed *in vitro* enzyme kinetics, using a previously described assay and recombinantly expressed and purified proteins [7, 54]. The total volume for each reaction was 50 μ L and contained 50 mM Bicine pH 9.0, 0.5 mM acCoA, 1 mM spermidine, 0.96 μ M SpeG enzyme, and/or 0.1 mM RcsB full-length protein. All reactions were initiated with 10 μ L of SpeG enzyme or enzyme dilution buffer (100 mM Bicine pH 9.0, 100 mM sodium chloride) and were performed in triplicate at 35°C for 20 min. To stop the reactions, 50 μ L of a solution containing 100 mM Tris HCl pH 8.0 and 6 M guanidine HCl was added to each reaction. To detect the product of the reaction (CoA), 200 μ L of a solution containing 0.2 mM 5,5'-Dithiobis(2-nitrobenzoic acid), 100 mM Tris HCl pH 8.0, and 1 mM EDTA was added to each reaction and incubated for 10 min at room temperature. The absorbance was then measured at 415 nm on a Biotek ELx808 microplate reader.

Surface plasmon resonance (SPR) analysis of binding interactions between SpeG and RcsB in absence or presence of spermidine

Binding interactions of *E. coli* SpeG to full-length *E. coli* RcsB or individual RcsB domains in the absence of spermidine were measured using a Reichert SR7500DC (Reichert Technologies, Buffalo, NY) dual channel spectrometer at the Keck Biophysics Facility at Northwestern University (Evanston IL, USA). Prior to immobilizing SpeG onto a carboxymethyl dextran hydrogel surface gold sensor chip (Reichert Technologies, Buffalo, NY), the surface of the chip containing COO⁻ groups were activated with a mixture of N-hydroxysuccinimide (NHS) and 1-ethyl-3-(3-dimethylaminopropyl)carbodiimide hydrochloride (EDC) to create amine reactive esters. SpeG protein (46 μ M) in solution containing 10 mM HEPES at pH 8.3 and 100 mM sodium chloride was then immobilized onto the chip and covalently coupled with the surface NHS esters at a flow rate of 40 μ L/min at room temperature. To achieve saturation, two sequential injections of SpeG for 3 min followed by 1.5 min of dissociation were performed. To block formation of residual NHS esters, an ethanolamine solution was injected over the chip. To remove weakly bound SpeG molecules, the chip was washed with running buffer containing 10 mM HEPES at pH 8.3 and 100 mM sodium chloride. The instrument was cooled and all SPR measurements were carried out at 4°C. All protein solutions were prepared in running buffer. 160 μ L of RcsB full-length (10, 21, 42, 53, 63 and 74 μ M), RcsB C-terminal domain (45, 67, 91, 114, 136, and 159 μ M), or RcsB N-terminal domain (59, 118, and 176 μ M) were injected sequentially over the SpeG-chip with a flow rate of 40 μ L min⁻¹ for 30 sec followed by a 1.5 min rinse and a 1 min dissociation. After each binding cycle, SpeG surfaces were regenerated by injecting 0.5 M sodium chloride for 45 sec at a flow rate of 30 μ L min⁻¹ and washed with running buffer. All analyte injections were performed in duplicate. For each measurement, a background response recorded in the reference cell was subtracted as well as the response from a blank injection with the running buffer.

To investigate how spermidine affects binding interactions of SpeG to RcsB and its individual domains, we used a Reichert4SR (Reichert Technologies, Buffalo, NY) four-channel SPR system at the Keck Biophysics Facility. SpeG was immobilized at a concentration of 46 μ M onto cells 3 and 4 using the amine coupling procedure described above. Cells 1 and 2 were

used as reference cells. All measurements were performed at 4°C. A solution containing 0.5 mM spermidine in the running buffer was flowed over the surface of the immobilized SpeG at 40 $\mu\text{L min}^{-1}$ for 30 sec followed by a 1.5 min rinse and a 1 min dissociation. The chip was then washed with running buffer until the SPR signal reached a stable value. 160 μL of RcsB full-length (10, 21, 42, 53, 63 and 74 μM), RcsB C-terminal domain (23, 45, 91, 114, and 136 μM) or RcsB N-terminal domain (59, 118, 177, 236 and 295 μM) were injected sequentially over the SpeG-chip, as described above, to monitor binding of RcsB constructs to SpeG in the presence of spermidine. After each binding cycle of RcsB full-length and RcsB C-terminal domain, SpeG surfaces were regenerated with an injection of 0.5 M sodium chloride for 1.5 min at a flow rate of 30 $\mu\text{L min}^{-1}$ and washed with the running buffer. Regeneration of the chip surface after injections of RcsB N-terminal domain was not required because the protein dissociated on its own. A background response for each run and the response from a blank injection were subtracted. With the exception of the RcsB N-terminal domain in the absence of spermidine, duplicate measurements were collected for each concentration of each protein. Data processing and kinetic analyses for all experiments were performed using TraceDrawer Data Analysis software (Reichert Technologies, Buffalo, NY).

SPR analysis of binding interactions between SpeG and the transcription factor RcsA

To examine binding interactions between SpeG and RcsB's auxiliary partner RcsA from *E. coli*, we used a four-channel SPR system at the Keck Biophysics Facility following the amine coupling protocol, as described above. SpeG protein at a concentration of 46 μM in 10 mM HEPES buffer at pH 8.3 containing 100 mM sodium chloride was immobilized onto the chip. 160 μL of RcsA protein solution in running buffer (21, 42, 64 and 85 μM) was injected consecutively over the SpeG-chip followed by regeneration and washing, as described above. A background response and response from a blank injection that contained running buffer were subtracted from each sensorgram to determine the actual binding response. Data were processed using TraceDrawer software.

Linear regression analysis

To determine whether experimental results were statistically significant, a linear regression was performed, comparing all experimental groups with their respective vector controls. All of the regressions used were set up as follows: the calculated *rprA* promoter activity was the response variable, the overexpressed plasmids or mutant were the explanatory variable, and time was a random effect. OD was not included as an effect on activity as it is already used in the calculation of activity. Time as a random effect was chosen based on the question asked: Accounting for the effects of time on activity does the experimental group in question significantly affect overall *rprA* promoter activity? The significance threshold was set at 0.05. The open source program R (version 3.3.2) and packages “lmerTest”, “ggplot2”, and “moments” were used to visualize and analyze the data (76,77,78,79).

Supporting information

S1 Fig. The effect of spermidine on *rprA* in the absence of SpeE. The *speE* mutant was transformed with either the VC or pSpeG and grown in TB7 supplemented with 50 μM IPTG and 0, 1.5, 2.5, or 5 mM spermidine. Growth and *rprA* promoter activity was measured over time. Each data point is an average of duplicate biological replicates and standard deviations. (PDF)

S2 Fig. Affinity analysis of RcsB binding to SpeG. (A) The maximum responses in the SPR sensograms for the first dilution series of RcsB C-terminal domain in the absence of spermidine are plotted against the analyte concentration. (B and C) The SPR sensograms for dilution series of RcsB full-length and its C-terminal domain after exposure to spermidine. The RcsB full-length or RcsB C-terminal domain protein was injected in five dilution series with the following concentrations: 21, 42, 53, 63 and 74 μ M (B) or 23, 45, 91, 114, and 136 μ M (C). The fitted data are shown in black.
(PDF)

S3 Fig. Phylogenetic tree of LuxR/FixJ DNA-binding domain of transcriptional regulators.

Phylogenetic tree was created in ClustalW2 server (<http://www.ebi.ac.uk/Tools/msa/clustalw2>). A list of 58 representatives of the conserved LuxR/FixJ DNA-binding domains was generated in NCBI server <http://www.ncbi.nlm.nih.gov/Structure/cdd> and includes DNA-binding domains of following transcriptional factors: RcsB from *Escherichia coli* (RcsB-Es_co) [GI:353570681], RcsB from *Erwinia amylovora* (RcsB-Er_am) [GI:33357861], YjjQ from *E. coli* (YjjQ-Es_co) [GI:83288197], BglJ from *E. coli* (BglJ-Es_co) [GI:3915634], YahA from *E. coli* (YahA-Es_co) [GI:2506596], YuaB from *E. coli* (YuaB-Es_co) [GI:81783897], DctR from *E. coli* (DctR-Es_co) [GI:57012697], RcsA from *E. coli* (RcsA-Es_co) [GI:60393000], EntR from *Citrobacter freundii* (EntR-Ci_fr) [GI:6015049], FimW from *Salmonella enterica* (FimW-Sa_en) [GI:585140], LuxR from *Bacteroides thetaiotaomicron* (LuxR-Ba_th) [GI:171849138], YgeK from *E. coli* (YgeK-Es_co) [GI:20140955], UhpA from *E. coli* (UhpA-Es_co) [GI:84029412], UvrY from *E. coli* (UvrY-Es_co) [GI:83288180], PA0034 from *Pseudomonas aeruginosa* (PA0034-Ps_ae) [GI:13959718], BvgA from *Bordetella pertussis* (BvgA-Bo_pe) [GI:61219948], FimZ from *E. coli* (FimZ-Es_co) [GI:84028128], EvgA from *E. coli* (EvgA-Es_co) [GI:82581667], FixJ from *Sinorhizobium meliloti* (FixJ-Si_me) [GI:159163516], StyR from *P. fluorescens* (StyR-Ps_fl) [GI:78100993], NodW from *Bradyrhizobium diazoefficiens* (NodW-Br_di) [GI:128495], Ycf29 from *Porphyra purpurea* (Ycf29-Po_pu) [GI:1723332], Ycf29 from *Cyanophora paradoxa* (Ycf29-Cy_pa) [GI:1351750], NarL from *E. coli* (NarL-Es_co) [GI:24158735], NarP from *E. coli* (NarP-Es_co) [GI:400374], GerE from *Bacillus subtilis* (GerE-Ba_su) [GI:13786948], VraR from *Staphylococcus aureus* (VraR-St_au) [GI:166007196], LiaR from *B. subtilis* (LiaR-Ba_su) [GI:68051995], DegU from *B. subtilis* (DegU-Ba_su) [GI:118438], YxjL from *B. subtilis* (YxjL-Ba_su) [GI:20141933], YhjB from *E. coli* (YhjB-Es_co) [GI:586682], CsgD from *E. coli* (CsgD-Es_co) [GI:1706166], MoaR from *Enterobacter aerogenes* (MoaR-En_ae) [GI:1709068], MalT from *E. coli* (MalT-Es_co) [GI:189028606], SgaR from *Hyphomicrobium methylovorum* (SgaR-Hy_me) [GI:6094276], Rv08090c from *Mycobacterium tuberculosis* (Rv08090c-My_tu) [GI:6137301], AgmR from *P. aeruginosa* (AgmR-Ps_ae) [GI:121420], AlkS from *P. oleovorans* (AlkS-Ps_ol) [GI:6226550], ComA from *B. subtilis* (ComA-Ba_su) [GI:116903], YdfI from *B. subtilis* (YdfI-Ba_su) [GI:68566110], ExeN from *Aeromonas salmonicida* (ExeN-Ae_sa) [GI:1175862], LuxR from *Aliivibrio fischeri* (LuxR-Al_fi) [GI:462556], VanR from *Vibrio anguillarum* (VanR-Vi_an) [GI:9297072], SolR from *Ralstonia solanacearum* (SolR-Ra_so) [GI:9297032], AhyR from *Aeromonas hydrophila* (AhyR-Ae_hy) [GI:61218504], LasR from *P. aeruginosa* (LasR-Ps_ae) [GI:125980], Y4HQ from *Sinorhizobium fredii* (Y4HQ-Si_fr) [GI:2495427], SdiA from *E. coli* (SdiA-Es_co) [GI:2506570], PhzR from *P. fluorescens* (PhzR-Ps_fl) [GI:2495423], CarR from *Pectobacterium carotovorum* (CarR-Pe_ca) [GI:2495418], YenR from *Yersinia enterocolitica* (YenR-Ye_en) [GI:1723596], RhiR from *Rhizobium leguminosarum* (RhiR-Rh_le) [GI:417645], TraR from *S. fredii* (TraR-Si_fr) [GI:158429605], MoxX from *Paracoccus denitrificans* (MoxX-Pa_de) [GI:266552], BrpA from *Streptomyces hygroscopicus* (BrpA-St_hy) [GI:231653], RaiR from *Rhizobium etli* (RaiR-Rh_et) [GI:9297035], TraR from *Agrobacterium tumefaciens* (TraR-Ag_tu) GI:23200109 and TraJ from *E. coli* (TraJ-Es_co)

[GI:464931].
(PDF)

S4 Fig. SPR analysis of SpeG and RcsA interaction. The SPR sensograms of SpeG and transcription regulator RcsA. The RcsA protein was injected in four dilution series. Duplicate measurements for each concentration indicated above SPR sensograms were performed.

(PDF)

Acknowledgments

We would like to thank the Keck Biophysics Facility at Northwestern University (Evanston, IL) for assistance with SPR data collection, Roberto Limeira and Cara Joyce (Loyola University Chicago) for the linear regression analyses of the *in vivo* data, Sarah Cook, David Christensen, and Bozena Zemaitaitis (Loyola University Chicago) for helping to complete and repeat the acetyltransferase overexpression experiments, and the members of the Visick and Wolfe labs (Loyola University Chicago) for important scientific discussions pertaining to this study.

Author Contributions

Conceptualization: Linda I. Hu, Ekaterina V. Filippova, Wayne F. Anderson, Misty L. Kuhn, Alan J. Wolfe.

Formal analysis: Linda I. Hu, Ekaterina V. Filippova, Misty L. Kuhn.

Funding acquisition: Wayne F. Anderson, Misty L. Kuhn, Alan J. Wolfe.

Investigation: Linda I. Hu, Ekaterina V. Filippova, Joseph Dang, Jiapeng Ruan, Misty L. Kuhn.

Resources: Sergii Pshenychnyi, Olga Kiryukhina.

Supervision: Wayne F. Anderson, Alan J. Wolfe.

Writing – original draft: Linda I. Hu, Ekaterina V. Filippova, Wayne F. Anderson, Misty L. Kuhn, Alan J. Wolfe.

Writing – review & editing: Linda I. Hu, Ekaterina V. Filippova, Wayne F. Anderson, Misty L. Kuhn, Alan J. Wolfe.

References

1. Fukuchi J, Kashiwagi K, Yamagishi M, Ishihama A, Igarashi K. Decrease in cell viability due to the accumulation of spermidine in spermidine acetyltransferase-deficient mutant of *Escherichia coli*. *The Journal of biological chemistry*. 1995; 270(32):18831–5. PMID: [7642535](#)
2. Limsuwun K, Jones PG. Spermidine acetyltransferase is required to prevent spermidine toxicity at low temperatures in *Escherichia coli*. *Journal of bacteriology*. 2000; 182(19):5373–80. PMID: [10986239](#)
3. Barbagallo M, Di Martino ML, Marcocci L, Pietrangeli P, De Carolis E, Casalino M, et al. A new piece of the *Shigella* Pathogenicity puzzle: spermidine accumulation by silencing of the *speG* gene [corrected]. *PLoS one*. 2011; 6(11):e27226. <https://doi.org/10.1371/journal.pone.0027226> PMID: [22102881](#)
4. Campilongo R, Di Martino ML, Marcocci L, Pietrangeli P, Leuzzi A, Grossi M, et al. Molecular and functional profiling of the polyamine content in enteroinvasive *E. coli*: looking into the gap between commensal *E. coli* and harmful *Shigella*. *PLoS one*. 2014; 9(9):e106589. <https://doi.org/10.1371/journal.pone.0106589> PMID: [25192335](#)
5. Joshi GS, Spontak JS, Klapper DG, Richardson AR. Arginine catabolic mobile element encoded *speG* abrogates the unique hypersensitivity of *Staphylococcus aureus* to exogenous polyamines. *Molecular microbiology*. 2011; 82(1):9–20. <https://doi.org/10.1111/j.1365-2958.2011.07809.x> PMID: [21902734](#)

6. Thurlow LR, Joshi GS, Clark JR, Spontak JS, Neely CJ, Maile R, et al. Functional modularity of the arginine catabolic mobile element contributes to the success of USA300 methicillin-resistant *Staphylococcus aureus*. *Cell host & microbe*. 2013; 13(1):100–7.
7. Filippova EV, Kuhn ML, Osipiuk J, Kiryukhina O, Joachimiak A, Ballicora MA, et al. A novel polyamine allosteric site of SpeG from *Vibrio cholerae* is revealed by its dodecameric structure. *Journal of molecular biology*. 2015; 427(6 Pt B):1316–34.
8. Fukuchi J, Kashiwagi K, Takio K, Igarashi K. Properties and structure of spermidine acetyltransferase in *Escherichia coli*. *The Journal of biological chemistry*. 1994; 269(36):22581–5. PMID: [8077207](#)
9. Sugiyama S, Ishikawa S, Tomitori H, Niiyama M, Hirose M, Miyazaki Y, et al. Molecular mechanism underlying promiscuous polyamine recognition by spermidine acetyltransferase. *The international journal of biochemistry & cell biology*. 2016; 76:87–97.
10. Filippova EV, Weigand S, Osipiuk J, Kiryukhina O, Joachimiak A, Anderson WF. Substrate-Induced Allosteric Change in the Quaternary Structure of the Spermidine N-Acetyltransferase SpeG. *Journal of molecular biology*. 2015; 427(22):3538–53. <https://doi.org/10.1016/j.jmb.2015.09.013> PMID: [26410587](#)
11. Majdalani N, Chen S, Murrow J, St John K, Gottesman S. Regulation of RpoS by a novel small RNA: the characterization of RprA. *Molecular microbiology*. 2001; 39(5):1382–94. PMID: [11251852](#)
12. Majdalani N, Hernandez D, Gottesman S. Regulation and mode of action of the second small RNA activator of RpoS translation, RprA. *Molecular microbiology*. 2002; 46(3):813–26. PMID: [12410838](#)
13. Bourret RB. Receiver domain structure and function in response regulator proteins. *Current opinion in microbiology*. 2010; 13(2):142–9. <https://doi.org/10.1016/j.mib.2010.01.015> PMID: [20211578](#)
14. Salazar ME, Laub MT. Temporal and evolutionary dynamics of two-component signaling pathways. *Current opinion in microbiology*. 2015; 24:7–14. <https://doi.org/10.1016/j.mib.2014.12.003> PMID: [25589045](#)
15. Jung K, Fried L, Behr S, Heermann R. Histidine kinases and response regulators in networks. *Current opinion in microbiology*. 2012; 15(2):118–24. <https://doi.org/10.1016/j.mib.2011.11.009> PMID: [22172627](#)
16. Majdalani N, Gottesman S. The Rcs phosphorelay: a complex signal transduction system. *Annual review of microbiology*. 2005; 59:379–405. <https://doi.org/10.1146/annurev.micro.59.050405.101230> PMID: [16153174](#)
17. Mariscotti JF, Garcia-Del Portillo F. Instability of the *Salmonella* RcsCDB signalling system in the absence of the attenuator IgaA. *Microbiology*. 2008; 154(Pt 5):1372–83. <https://doi.org/10.1099/mic.0.2007/015891-0> PMID: [18451046](#)
18. Castanie-Cornet MP, Cam K, Jacq A. RcsF is an outer membrane lipoprotein involved in the RcsCDB phosphorelay signaling pathway in *Escherichia coli*. *Journal of bacteriology*. 2006; 188(12):4264–70. <https://doi.org/10.1128/JB.00004-06> PMID: [16740933](#)
19. Cho SH, Szweczyk J, Pesavento C, Zietek M, Banzhaf M, Roszczenko P, et al. Detecting envelope stress by monitoring beta-barrel assembly. *Cell*. 2014; 159(7):1652–64. <https://doi.org/10.1016/j.cell.2014.11.045> PMID: [25525882](#)
20. Konovalova A, Perlman DH, Cowles CE, Silhavy TJ. Transmembrane domain of surface-exposed outer membrane lipoprotein RcsF is threaded through the lumen of beta-barrel proteins. *Proceedings of the National Academy of Sciences of the United States of America*. 2014; 111(41):E4350–8. <https://doi.org/10.1073/pnas.1417138111> PMID: [25267629](#)
21. Mariscotti JF, Garcia-del Portillo F. Genome expression analyses revealing the modulation of the *Salmonella* Rcs regulon by the attenuator IgaA. *Journal of bacteriology*. 2009; 191(6):1855–67. <https://doi.org/10.1128/JB.01604-08> PMID: [19124574](#)
22. Hussein NA, Cho SH, Laloux G, Siam R, Collet JF. Distinct domains of *Escherichia coli* IgaA connect envelope stress sensing and down-regulation of the Rcs phosphorelay across subcellular compartments. *PLoS Genet*. 2018; 14(5):e1007398. <https://doi.org/10.1371/journal.pgen.1007398> PMID: [29852010](#)
23. Pucciarelli MG, Rodriguez L, Garcia-Del Portillo F. A Disulfide Bond in the Membrane Protein IgaA Is Essential for Repression of the RcsCDB System. *Front Microbiol*. 2017; 8:2605. <https://doi.org/10.3389/fmicb.2017.02605> PMID: [29312270](#)
24. Sato T, Takano A, Hori N, Izawa T, Eda T, Sato K, et al. Role of the inner-membrane histidine kinase RcsC and outer-membrane lipoprotein RcsF in the activation of the Rcs phosphorelay signal transduction system in *Escherichia coli*. *Microbiology*. 2017; 163(7):1071–80. <https://doi.org/10.1099/mic.0.000483> PMID: [28691662](#)
25. Fredericks CE, Shibata S, Aizawa S, Reimann SA, Wolfe AJ. Acetyl phosphate-sensitive regulation of flagellar biogenesis and capsular biosynthesis depends on the Rcs phosphorelay. *Molecular microbiology*. 2006; 61(3):734–47. <https://doi.org/10.1111/j.1365-2958.2006.05260.x> PMID: [16776655](#)

26. Howery KE, Clemmer KM, Rather PN. The Rcs regulon in *Proteus mirabilis*: implications for motility, biofilm formation, and virulence. *Current genetics*. 2016.
27. Lehti TA, Heikkinen J, Korhonen TK, Westerlund-Wikstrom B. The response regulator RcsB activates expression of Mat fimbriae in meningitic *Escherichia coli*. *Journal of bacteriology*. 2012; 194(13):3475–85. <https://doi.org/10.1128/JB.06596-11> PMID: 22522901
28. Wang Q, Harshey RM. Rcs signalling-activated transcription of *rscA* induces strong anti-sense transcription of upstream *fliPQR* flagellar genes from a weak intergenic promoter: regulatory roles for the anti-sense transcript in virulence and motility. *Molecular microbiology*. 2009; 74(1):71–84. <https://doi.org/10.1111/j.1365-2958.2009.06851.x> PMID: 19703110
29. Hu LI, Chi BK, Kuhn ML, Filippova EV, Walker-Peddakotla AJ, Basell K, et al. Acetylation of the response regulator RcsB controls transcription from a small RNA promoter. *Journal of bacteriology*. 2013; 195(18):4174–86. <https://doi.org/10.1128/JB.00383-13> PMID: 23852870
30. Francez-Charlot A, Laugel B, Van Gemert A, Dubarry N, Wiorowski F, Castanie-Cornet MP, et al. RcsCDB His-Asp phosphorelay system negatively regulates the *fliHDC* operon in *Escherichia coli*. *Molecular microbiology*. 2003; 49(3):823–32. PMID: 12864862
31. Filippova EV, Zemaitaitis B, Aung T, Wolfe AJ, Anderson WF. Structural Basis for DNA Recognition by the Two-Component Response Regulator RcsB. *MBio*. 2018; 9(1).
32. Pristovsek P, Sengupta K, Lohr F, Schafer B, von Trebra MW, Ruterjans H, et al. Structural analysis of the DNA-binding domain of the *Erwinia amylovora* RcsB protein and its interaction with the RcsAB box. *The Journal of biological chemistry*. 2003; 278(20):17752–9. <https://doi.org/10.1074/jbc.M301328200> PMID: 12740396
33. Wehland M, Bernhard F. The RcsAB box. Characterization of a new operator essential for the regulation of exopolysaccharide biosynthesis in enteric bacteria. *The Journal of biological chemistry*. 2000; 275(10):7013–20. PMID: 10702265
34. Castanie-Cornet MP, Cam K, Bastiat B, Cros A, Bordes P, Gutierrez C. Acid stress response in *Escherichia coli*: mechanism of regulation of *gadA* transcription by RcsB and GadE. *Nucleic acids research*. 2010; 38(11):3546–54. <https://doi.org/10.1093/nar/gkq097> PMID: 20189963
35. Pannen D, Fabisch M, Gausling L, Schnetz K. Interaction of the RcsB Response Regulator with Auxiliary Transcription Regulators in *Escherichia coli*. *The Journal of biological chemistry*. 2016; 291(5):2357–70. <https://doi.org/10.1074/jbc.M115.696815> PMID: 26635367
36. Stratmann T, Pul U, Wurm R, Wagner R, Schnetz K. RcsB-BglJ activates the *Escherichia coli* *leuO* gene, encoding an H-NS antagonist and pleiotropic regulator of virulence determinants. *Molecular microbiology*. 2012; 83(6):1109–23. <https://doi.org/10.1111/j.1365-2958.2012.07993.x> PMID: 22295907
37. Kuhne C, Singer HM, Grabisch E, Codutti L, Carlomagno T, Scrima A, et al. RflM mediates target specificity of the RcsCDB phosphorelay system for transcriptional repression of flagellar synthesis in *Salmonella enterica*. *Molecular microbiology*. 2016; 101(5):841–55. <https://doi.org/10.1111/mmi.13427> PMID: 27206164
38. Nassif X, Honore N, Vasselon T, Cole ST, Sansonetti PJ. Positive control of colanic acid synthesis in *Escherichia coli* by *rmpA* and *rmpB*, two virulence-plasmid genes of *Klebsiella pneumoniae*. *Molecular microbiology*. 1989; 3(10):1349–59. PMID: 2693894
39. Mouslim C, Latifi T, Groisman EA. Signal-dependent requirement for the co-activator protein RcsA in transcription of the RcsB-regulated *ugd* gene. *The Journal of biological chemistry*. 2003; 278(50):50588–95. <https://doi.org/10.1074/jbc.M309433200> PMID: 14514676
40. Thao S, Chen CS, Zhu H, Escalante-Semerena JC. Nepsilon-lysine acetylation of a bacterial transcription factor inhibits its DNA-binding activity. *PloS one*. 2010; 5(12):e15123. <https://doi.org/10.1371/journal.pone.0015123> PMID: 21217812
41. Kuhn ML, Zemaitaitis B, Hu LI, Sahu A, Sorensen D, Minasov G, et al. Structural, kinetic and proteomic characterization of acetyl phosphate-dependent bacterial protein acetylation. *PloS one*. 2014; 9(4):e94816. <https://doi.org/10.1371/journal.pone.0094816> PMID: 24756028
42. Schilling B, Christensen D, Davis R, Sahu AK, Hu LI, Walker-Peddakotla A, et al. Protein acetylation dynamics in response to carbon overflow in *Escherichia coli*. *Molecular microbiology*. 2015; 98(5):847–63. <https://doi.org/10.1111/mmi.13161> PMID: 26264774
43. Weinert BT, Iesmantavicius V, Wagner SA, Scholz C, Gummeson B, Beli P, et al. Acetyl-phosphate is a critical determinant of lysine acetylation in *E. coli*. *Molecular cell*. 2013; 51(2):265–72. <https://doi.org/10.1016/j.molcel.2013.06.003> PMID: 23830618
44. Hentchel KL, Escalante-Semerena JC. Acylation of Biomolecules in Prokaryotes: a Widespread Strategy for the Control of Biological Function and Metabolic Stress. *Microbiology and molecular biology reviews: MMBR*. 2015; 79(3):321–46. <https://doi.org/10.1128/MMBR.00020-15> PMID: 26179745

45. Wolfe AJ. Bacterial protein acetylation: new discoveries unanswered questions. *Current genetics*. 2016; 62(2):335–41. <https://doi.org/10.1007/s00294-015-0552-4> PMID: 26660885
46. Ren J, Sang Y, Tan Y, Tao J, Ni J, Liu S, et al. Acetylation of Lysine 201 Inhibits the DNA-Binding Ability of PhoP to Regulate Salmonella Virulence. *PLoS pathogens*. 2016; 12(3):e1005458. <https://doi.org/10.1371/journal.ppat.1005458> PMID: 26943369
47. Castano-Cerezo S, Bernal V, Post H, Fuhrer T, Cappadona S, Sanchez-Diaz NC, et al. Protein acetylation affects acetate metabolism, motility and acid stress response in *Escherichia coli*. *Molecular systems biology*. 2014; 10:762. <https://doi.org/10.15252/msb.20145227> PMID: 25518064
48. Datsenko KA, Wanner BL. One-step inactivation of chromosomal genes in *Escherichia coli* K-12 using PCR products. *Proceedings of the National Academy of Sciences of the United States of America*. 2000; 97(12):6640–5. <https://doi.org/10.1073/pnas.120163297> PMID: 10829079
49. Baba T, Ara T, Hasegawa M, Takai Y, Okumura Y, Baba M, et al. Construction of *Escherichia coli* K-12 in-frame, single-gene knockout mutants: the Keio collection. *Molecular systems biology*. 2006; 2:2006 0008.
50. Dieckman L, Gu M, Stols L, Donnelly MI, Collart FR. High throughput methods for gene cloning and expression. *Protein expression and purification*. 2002; 25(1):1–7. <https://doi.org/10.1006/prev.2001.1602> PMID: 12071692
51. Kitagawa M, Ara T, Arifuzzaman M, Ioka-Nakamichi T, Inamoto E, Toyonaga H, et al. Complete set of ORF clones of *Escherichia coli* ASKA library (a complete set of *E. coli* K-12 ORF archive): unique resources for biological research. *DNA research: an international journal for rapid publication of reports on genes and genomes*. 2005; 12(5):291–9.
52. Stols L, Gu M, Dieckman L, Raffin R, Collart FR, Donnelly MI. A new vector for high-throughput, ligation-independent cloning encoding a tobacco etch virus protease cleavage site. *Protein expression and purification*. 2002; 25(1):8–15. <https://doi.org/10.1006/prev.2001.1603> PMID: 12071693
53. Eschenfeldt WH, Makowska-Grzyska M, Stols L, Donnelly MI, Jedrzejczak R, Joachimiak A. New LIC vectors for production of proteins from genes containing rare codons. *J Struct Funct Genomics*. 2013; 14(4):135–44. <https://doi.org/10.1007/s10969-013-9163-9> PMID: 24057978
54. Kuhn ML, Majorek KA, Minor W, Anderson WF. Broad-substrate screen as a tool to identify substrates for bacterial Gcn5-related N-acetyltransferases with unknown substrate specificity. *Protein science: a publication of the Protein Society*. 2013; 22(2):222–30.
55. Majorek KA, Kuhn ML, Chruszcz M, Anderson WF, Minor W. Structural, functional, and inhibition studies of a Gcn5-related N-acetyltransferase (GNAT) superfamily protein PA4794: a new C-terminal lysine protein acetyltransferase from *Pseudomonas aeruginosa*. *The Journal of biological chemistry*. 2013; 288(42):30223–35. <https://doi.org/10.1074/jbc.M113.501353> PMID: 24003232
56. Majorek KA, Osinski T, Tran DT, Revilla A, Anderson WF, Minor W, et al. Insight into the 3D structure and substrate specificity of previously uncharacterized GNAT superfamily acetyltransferases from pathogenic bacteria. *Biochim Biophys Acta*. 2017; 1865(1):55–64.
57. Vetting MW, Bareich DC, Yu M, Blanchard JS. Crystal structure of RimI from *Salmonella typhimurium* LT2, the GNAT responsible for N(alpha)-acetylation of ribosomal protein S18. *Protein Sci*. 2008; 17(10):1781–90. <https://doi.org/10.1110/ps.035899.108> PMID: 18596200
58. Stout V, Gottesman S. RcsB and RcsC: a two-component regulator of capsule synthesis in *Escherichia coli*. *Journal of bacteriology*. 1990; 172(2):659–69. PMID: 2404948
59. Altschul SF, Madden TL, Schaffer AA, Zhang J, Zhang Z, Miller W, et al. Gapped BLAST and PSI-BLAST: a new generation of protein database search programs. *Nucleic acids research*. 1997; 25(17):3389–402. PMID: 9254694
60. Brill JA, Quinlan-Walsh C, Gottesman S. Fine-structure mapping and identification of two regulators of capsule synthesis in *Escherichia coli* K-12. *Journal of bacteriology*. 1988; 170(6):2599–611. PMID: 2836365
61. Majdalani N, Heck M, Stout V, Gottesman S. Role of RcsF in signaling to the Rcs phosphorelay pathway in *Escherichia coli*. *Journal of bacteriology*. 2005; 187(19):6770–8. <https://doi.org/10.1128/JB.187.19.6770-6778.2005> PMID: 16166540
62. Pruss BM, Besemann C, Denton A, Wolfe AJ. A complex transcription network controls the early stages of biofilm development by *Escherichia coli*. *Journal of bacteriology*. 2006; 188(11):3731–9. <https://doi.org/10.1128/JB.01780-05> PMID: 16707665
63. Laubacher ME, Ades SE. The Rcs phosphorelay is a cell envelope stress response activated by peptidoglycan stress and contributes to intrinsic antibiotic resistance. *Journal of bacteriology*. 2008; 190(6):2065–74. <https://doi.org/10.1128/JB.01740-07> PMID: 18192383
64. Richter L, Johnston A, Lam A. The Rcs Phosphorelay System and RcsB Regulated *rprA* Contribute to Intrinsic Antibiotic Resistance in *Escherichia coli* Exposed to Antibiotics Targeting the Cell Wall. *J Exper Microbiol and Immunol*. 2016; 2:42–8.

65. Chattopadhyay MK, Keembiyehetty CN, Chen W, Tabor H. Polyamines Stimulate the Level of the sigma38 Subunit (RpoS) of Escherichia coli RNA Polymerase, Resulting in the Induction of the Glutamate Decarboxylase-dependent Acid Response System via the gadE Regulon. *The Journal of biological chemistry*. 2015; 290(29):17809–21. <https://doi.org/10.1074/jbc.M115.655688> PMID: 26025365
66. Castanie-Cornet MP, Treffandier H, Francez-Charlot A, Gutierrez C, Cam K. The glutamate-dependent acid resistance system in Escherichia coli: essential and dual role of the His-Asp phosphorelay RcsCDB/AF. *Microbiology*. 2007; 153(Pt 1):238–46. <https://doi.org/10.1099/mic.0.29278-0> PMID: 17185552
67. Carper SW, Willis DG, Manning KA, Gerner EW. Spermidine acetylation in response to a variety of stresses in Escherichia coli. *The Journal of biological chemistry*. 1991; 266(19):12439–41. PMID: 2061318
68. Silhavy TJ, Berman M. L., and Enquist L. W. *Experiments with gene fusions*. Cold Spring Harbor, NY: Cold Spring Harbor Laboratory; 1984.
69. Powell BS, Rivas MP, Court DL, Nakamura Y, Turnbough CL Jr. Rapid confirmation of single copy lambda prophage integration by PCR. *Nucleic acids research*. 1994; 22(25):5765–6. PMID: 7838735
70. Hanahan D. Studies on transformation of Escherichia coli with plasmids. *Journal of molecular biology*. 1983; 166(4):557–80. PMID: 6345791
71. Chung CT, Niemela SL, Miller RH. One-step preparation of competent Escherichia coli: transformation and storage of bacterial cells in the same solution. *Proceedings of the National Academy of Sciences of the United States of America*. 1989; 86(7):2172–5. PMID: 2648393
72. Anderson WFE. *Structural Genomics and Drug Discovery. Methods and Protocols*. 1 ed: Humana Press; 2014. 344 p.
73. Kwon K, Peterson SN. High-throughput cloning for biophysical applications. *Methods in molecular biology*. 2014; 1140:61–74. https://doi.org/10.1007/978-1-4939-0354-2_5 PMID: 24590709
74. Makowska-Grzyska M, Kim Y, Maltseva N, Li H, Zhou M, Joachimiak G, et al. Protein production for structural genomics using E. coli expression. *Methods in molecular biology*. 2014; 1140:89–105. https://doi.org/10.1007/978-1-4939-0354-2_7 PMID: 24590711
75. Kuhn ML, Majorek KA, Minor W, Anderson WF. Broad-substrate screen as a tool to identify substrates for bacterial Gcn5-related N-acetyltransferases with unknown substrate specificity. *Protein Science*. 2013; 22(2):222–30. <https://doi.org/10.1002/pro.2199> PMID: 23184347